Journal of Archaeological Science: Reports 11 (2017) 600–612

Contents lists available at ScienceDirect

Journal of Archaeological Science: Reports

journal homepage: www.elsevier.com/locate/jasrep

Analyses of glass tesserae from Kilise Tepe: New insights into an early Byzantine production technology

Elisabetta Neri [a,*], Mark Jackson [b], Margaret O'Hea [c], Tom Gregory [d], Maryse Blet-Lemarquand [a], Nadine Schibille [a,*]

[a] IRAMAT-CEP, UMR5060, CNRS/Université d'Orléans, 3D rue de la Férollerie, CS 60061, 45071 Orléans CEDEX 2, France
[b] Newcastle University, School of History, Classics and Archaeology, Armstrong Building, Newcastle upon Tyne NE1 7RU, United Kingdom
[c] Classics, Archaeology and Ancient History, School of Humanities, The University of Adelaide, 5005, Australia
[d] Institute of Archaeology, UCL, 31-34 Gordon Square, London WC1H 0PY, United Kingdom

ARTICLE INFO

Article history:
Received 20 October 2016
Received in revised form 23 December 2016
Accepted 27 December 2016
Available online xxxx

Keywords:
Mosaics
Byzantine glass tesserae
Asia Minor
Calcium phosphate
Lead stannate
Foy-2
Levantine I

ABSTRACT

There is substantial archaeological evidence to suggest that glass mosaics were ubiquitous throughout late antique and Byzantine Asia Minor. However, issues about the manufacture of Byzantine glass tesserae, the diffusion of their technology and the economic implications have been little discussed. This paper presents the results of the analytical and technological investigation of 28 glass fragments from Kilise Tepe (Cilicia, Turkey), including 22 tesserae, 3 gilded plaques and 1 fragment of a window, a vessel and an ingot. The samples were analysed by EPMA, LA-ICP-MS and SEM-EDS. Two different base glasses from different primary production sites were used in the production of the glass: Foy-2 probably from Egypt, and Levantine I produced in Syro-Palestine. Variations in the chemical fingerprint and morphology of crystalline particles reveal differences in the colouring and opacifying techniques that may point to multiple secondary production sites. Whereas the red samples show signs of in situ crystallization of metallic copper, ready-made lead stannate was added as yellow pigment for the colouring of the green and yellow tesserae. In addition, calcium phosphate particles, likely deriving from bone-ash, were found in one turquoise specimen. When compared with other late antique sites, our results testify to changes in the Roman centralized production tradition and a diversification of supply and secondary manufacturing practices of mosaic tesserae.

1. Introduction

Recent scientific studies have highlighted technological changes in the use of fluxing agents and sand sources, offering an opportunity to trace the chronological and geographical developments in the manufacture of raw glass (e.g. Bayley et al., 2015; Schibille et al., 2016a; Degryse, 2014). Much less is known about the practices of secondary workshops, how and where, for example, the raw glass was opacified, coloured and transformed into mosaic tesserae. Therefore, it is still unknown whether the secondary production of tesserae was a centralized affair, where one workshop produced tesserae of varying colours, or whether multiple workshops specialised in one colour at the time (Schibille et al., 2012). The systematic study of the opacifying and colouring agents in conjunction with the primary glass production groups can provide valuable insights into the diffusion of specific techniques and by extension into the organization of production and supply at consumer sites. A comparative analysis of glass tesserae, whether loose or still in situ, can identify potential markers for craft practices and trading networks and help to refine the chronology of production technologies and materials (James, 2006; James et al., 2013; Neri, 2016).

Wall and vault mosaics that consist predominantly of glass tesserae were evidently a common form of architectural decoration and more widespread during the late antique and Byzantine periods than has previously been recognized (e.g. James et al., 2013, and the database http://www.sussex.ac.uk/byzantine/mosaic/). In Asia Minor in particular, glass mosaics have been found in a variety of archaeological contexts and states of preservation, including mosaic decorations still in situ as well as fragments and loose tesserae from archaeological excavations (Fig. 1). However, only few of these mosaics and their materials have been analysed. Some studies of loose tesserae from sites in Asia Minor have been published and include wall mosaics from Hagia Sophia (Moropoulou et al., 2016) and Hagios Polyeuktos at Constantinople (Schibille and McKenzie, 2014), Sagalassos (Schibille et al., 2012) and Amorium (Wypyski, 2005), and the wall mosaics from geographically related regions such as Cyprus (Bonnerot et al., 2016) and Huarte in northern Syria (Lahanier, 1987). Glass tesserae from some floor mosaics were studied from Tyana (Lachin et al., 2009; Silvestri et al., 2016) and Antioch (Wypyski and Becker, 2004). Most of these studies discuss the

* Corresponding authors.
E-mail addresses: eneri@cnrs-orleans.fr (E. Neri), nadine.schibille@cnrs-orleans.fr (N. Schibille).

http://dx.doi.org/10.1016/j.jasrep.2016.12.036
2352-409X/

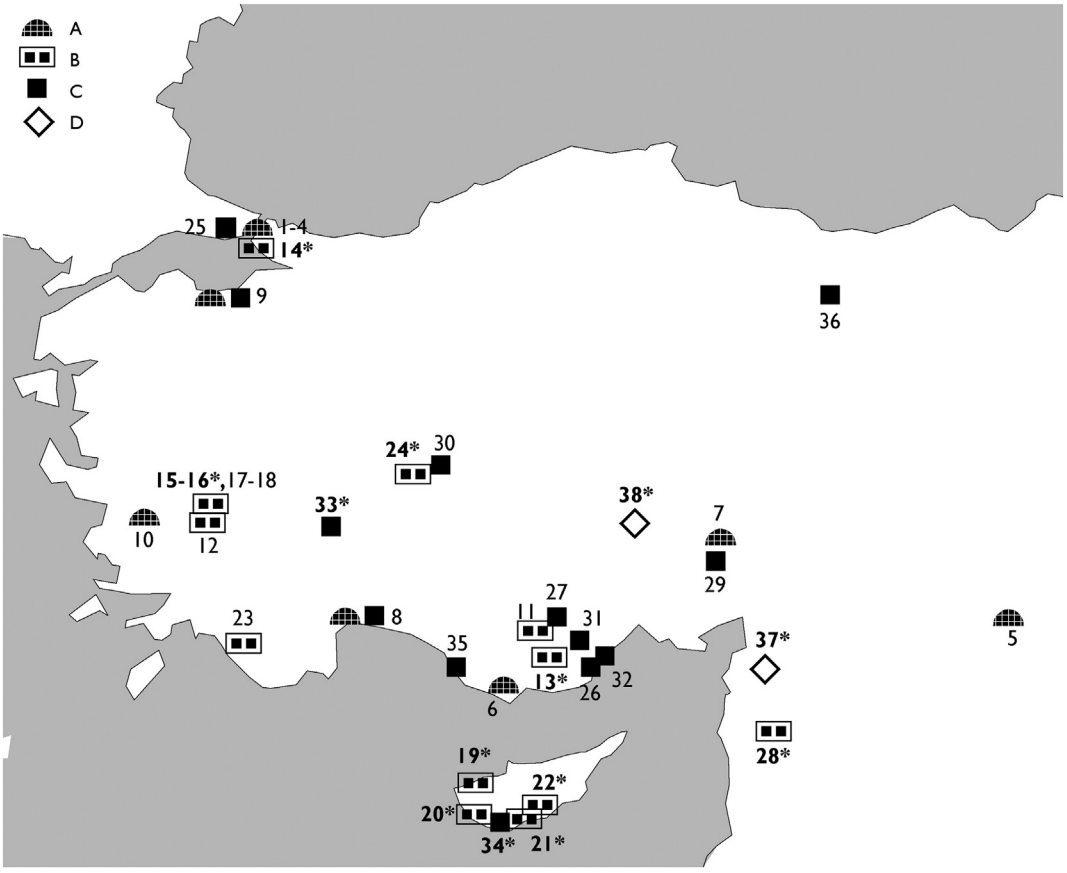

Fig. 1. Map of wall mosaic findings in Asia Minor and Cyprus. Asterisks indicate the sites with analyses of glass tesserae (literature in James et al., 2013 and Neri, 2016). A. In situ mosaics: 1. Constantinople, St. Sophia, 6th and 9th c.; 2. Constantinople, St. Irene, 6th and 8th c.; 3. Sts. Sergius and Bacchus, 6th c.; 4. Constantinople, Kalenderhane Camii, 6th c.; 5. Mar Gabriel, Sts. Samuel, Simeon, Gabriel and Kartmin, 6th c.; Anemurium, baths' church (building III, 5), 6th c.; 7. Ferhatlı Köyü, Akhiza cathedral, 6th c.; 8. Antalya, Cumanin Camii, 6th-7th c.; 9. Trigleia, St. Stephen, 8th c.; 10. Dereağzi, church, 9th–10th c. B. Mosaics in collapse layers: 11 Alahan, St. John the Evangelist, 5th c.; 12. Laodicea, Cathedral, 5th-6th c.; 13. Kilise Tepe, 5th-6th c.; 14. Constantinople, St. Polyeuktos, 6th c.; 15. Hierapolis, St. Philip, 6th and 9th c.; 16. Hierapolis, church near the theatre, 6th c.; 17. Hierapolis, Martyrion, 6th c.; 18. Hierapolis, church near the commercial agora, 6th c.; 19. Polis Chrysochous, 6th c.; 20. Yeroskipou, Ayioi Pente, 6th c.; 21. Amathous, Acropolis basilica, 6th c.; 22. Kalavasos-Kopetra, 6th c.; 23. Xanthos, baptistery, 7th c.; 24. Amorium, lower city church, 10th c. C. Tesserae in collapse layers: 25. Constantinople, St. John of Studios, 5th and 10th c.; 26. Corycus, transept church, 5th c.; 27. Dag Pazari, church, 5th c.; 28. Huarte, Photios Church, 5th c.; 13. Kilise Tepe, 5th-6th c.; 29. Anazarbus, Rock-cut Church, 5th-6th c.; 30. Germia, St. Michael, 5th-6th c.; 31. Ura, town church, 5th-6th c.; 32. Yemiskum, church 1, 5th-6th c.; 33. Sagalassos, basilica in the temple of Apollo Clarius, 5th-6th c.; 34. Kourion,, 6th c.; 8. Antalya, Cumanin Camii, 6th-7th c.; 35. Halil Limani, church, 6th-7th c.; 9.Trigleia, St. Stephen, 8th c.; 36. Koloneia, Mavrokastron-Karahisar, 9th-10th c. D. Floor mosaics with glass tesserae (comparative analyses): 37. Antioch, 4th c.; 38. Tyana, 5th c.

data of only a single context without providing an integrated view by comparing the data to other assemblages.

The primary aim of the present study is to characterize the chemical composition and microstructure of the glass mosaic tesserae from Kilise Tepe (Cilicia) in order to determine the provenance of the base glass and their opacifying and colouring techniques. By comparing the Kilise Tepe data to those of other published glass tesserae from late antique contexts, we explore the chronological and geographical spread of these techniques. This in turn enables the identification of commercial and technological networks that underlie the production and supply of glass tesserae in early Byzantine Asia Minor.

1.1. Archaeological context

Kilise Tepe is located on a terrace above the Göksu river that links central Anatolia to the Mediterranean at Seleucia, the metropolis of Isauria. Occupation of the site is attested from the Early Bronze Age through to the 13th century CE (Postgate and Thomas, 2007). Excavations carried out during the 1990s and reinitiated in 2007 have unearthed a Byzantine church and a rural settlement, with vernacular structures (Postgate and Thomas, 2007; Jackson, 2013, 2015). Judging from the ceramic finds, Kilise Tepe appears to have been well connected and part of a larger exchange network during the Roman and late antique period, even though it remained a relatively small settlement. In addition to the local production of water jars, imported wares such as late Roman amphorae from the coastal zone of Cilicia and western Asia Minor have been recovered as well as some examples of red slip ware from Africa Proconsularis (Jackson, 2015). What is more, the 1990s excavations of the Byzantine church and its immediate surroundings yielded almost a thousand loose glass tesserae, reflecting Kilise Tepe's prosperity at the time (Jackson, 2007, 2013). The tesserae were retrieved mostly from inside the early Byzantine church, specifically in the apse, the *templon* area, the north aisle as well as in the narthex. They typically come from filling and levelling layers that preceded the construction of the middle Byzantine church (12th–13th CE). A group of 767 tesserae was found at the east end of the north aisle of the church together with broken glass (Collon, 2007). The tesserae were found mixed also with the powdery remains of mortar and were at first considered by the excavator to represent a fallen wall mosaic. The context from which they came lay above the robbed floor of the church and they were associated with a discrete area of chipped fragments of marble caused by the breaking up of marble blocks (Jackson, 2007: 190). This context suggests that the tesserae may have been a collection of re-usable material after the destruction of the early Byzantine edifice. Similar practices have been observed in numerous other late antique churches (e.g. Keller, 2006).

It is thus assumed that the tesserae belonged to the decoration of the late antique church. The foundation of the church can be attributed to

the second half of the fourth century based on the range of lamps recovered. The earliest well-dated lamp from the church is a prunted conical beaker that has been attributed to the fourth century (O'Hea, 2016: 283–284). Additions or major replacements seem to have occurred in the late fifth century, judging from goblet lamps and hollow-stemmed hanging lamps in metal polykandela. The circumstantial evidence provides a tentative dating for the use of the early Byzantine church and its mosaics between the late fourth and early seventh century CE.

The glass tesserae are generally of small dimensions (0.7–1 cm) and the colours include gold, blue, turquoise, green, red and black. The abundance of gold leaf tesserae (45%) strongly suggests their use for extensive gold backgrounds. The prevalence of greens, turquoise and blues is most likely indicative of the depiction of vegetable motifs and water elements in analogy to other late antique and early medieval mosaic decorations. In addition to the tesserae, 13 fragments of rectangular greenish glass slabs with gold foil under a protective thin layer of colourless glass were found immediately south of the church as well as scattered across the site. None was complete, but corners survive (Fig. 2a); the largest were > 4 cm in side length and at least 0.4 cm thick. All had thickened and semi-folded edges. A grey mortar or grout was evenly applied to the back of each, which might simply be the remains from forming the slabs in molds and which may have served to accentuate the gilded effect rather than indicating pre-use, as has been observed elsewhere (e.g. Neri, 2016). As such, these gilded plaques were probably the semi-finished products for the manufacture of some of the gold leaf tesserae often found in association with the gilded plaques. This interpretation is further corroborated by the fact that both, the gold leaf tesserae and the gilded plaques, show the same rounded and thick edges. The coloured tesserae were, instead, manufactured from bun-shaped ingots or glass-cakes (Fig. 2b). The fact that gilded plaques and fragments of coloured ingots were found provides evidence that at least some of the tesserae were cut on site.

1.2. Materials

The 22 tesserae and three gilded plaques as well as the ingot, vessel and window glass fragments under investigation in this study were unearthed during the 2007 campaign from outside the church and cover the full range of colours (Table 1, Fig. 3). Most of the gold leaf tesserae preserve only the support and, in some cases, fragments of the gold leaf. The base of the gold leaf tesserae tends to be slightly amber or greenish in colour. The blue tesserae are typically translucent. The lighter shades of blue exhibit a more heterogeneous structure with many bubbles (Fig. 4a) compared to the darker cobalt blue samples (Fig. 4b). The majority of the green and turquoise tesserae are more or less opaque. The green samples have particles of yellow pigment

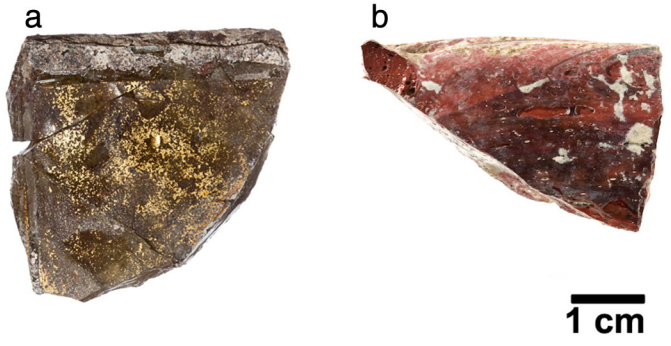

Fig. 2. Intermediate semi-finished material for mosaic production. (a) corner of gilded plaques with rounded edges; (b) cake-shaped red glass ingot. (For interpretation of the references to colour in this figure legend, the reader is referred to the web version of this article.)

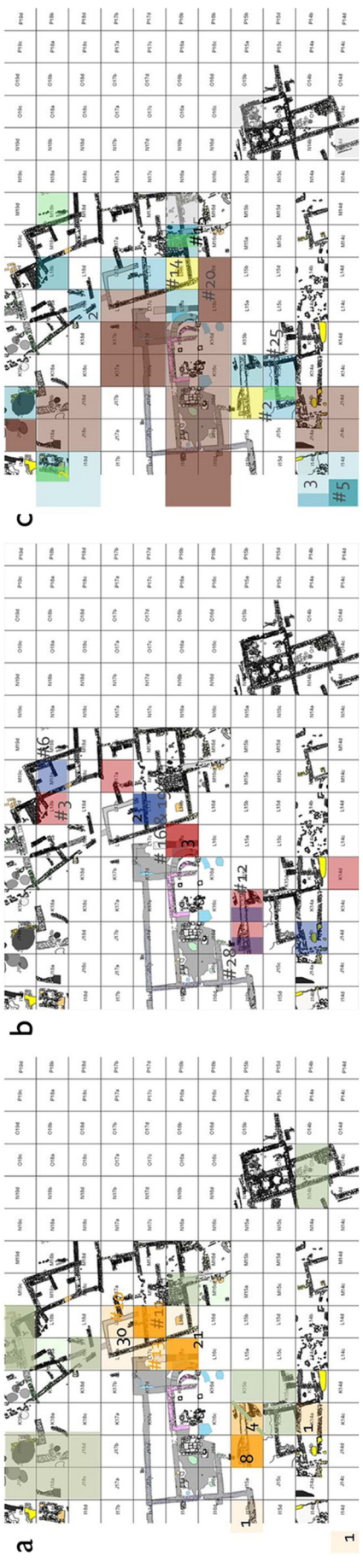

Fig. 3. Plan of the Kilise Tepe Byzantine church complex. Find spots of the different tesserae: (a) gold tesserae and gilded plaques; (b) yellow, green and turquoise tesserae; (c) red and cobalt blue tesserae. (For interpretation of the references to colour in this figure legend, the reader is referred to the web version of this article.)

(Fig. 4c) or clay inclusions dispersed in the glass matrix (Fig. 4d). The red tesserae are either relatively homogeneous (Fig. 4e) or they show layerings of green transparent and red glass (Fig. 4f).

2. Methods

The 28 samples were analysed by electron probe microanalysis (EPMA) and laser ablation inductively coupled plasma mass spectrometry (LA-ICP-MS) to establish their major, minor and trace element patterns. The coloured and opaque tesserae were additionally examined by scanning electron microscopy with energy dispersive X-ray spectrometry (SEM-EDS). Small glass fragments were mounted in epoxy resin and polished with a series of diamond pastes down to 0.25 μm. Polished blocks were carbon-coated using a Quorum K975X high vaccuum thermal evaporator coater.

2.1. EPMA

The polished and carbon coated blocks were analysed at the Institute of Archaeology, UCL, using a JEOL JXA 8100 microprobe with three wavelength dispersive X-ray spectrometers (see e.g. Freestone et al., 2015). The operating conditions were set at 15 kV accelerating voltage with a beam current of 50 nA, the beam diameter set to "0", a working distance of 11 mm and a magnification of 800×, resulting in a raster area of approximately 150 by 110 μm. Three areas were thus analysed on each sample. Counting times were 30s on peak and 10s on background. To monitor the precision and accuracy of the analyses, Corning Museum ancient glass standards A and B (Brill, 1999) were measured at the beginning and end of each run. The results compare well with the given values and accuracy is within <5% for most major and minor elements except for titanium, iron, copper and manganese (Table S1).

2.2. LA-ICP-MS

The polished cross-sections were additionally examined by LA-ICP-MS at the Centre Ernest-Babelon of the IRAMAT (Orléans) (Gratuze, 2016; Schibille et al., 2016b). The 193 nm laser was operated at an energy of 5 mJ, a pulse frequency of 10 Hz and a spot size diameter of 100 μm. The procedure consisted of 20 s pre-ablation time, followed by 50 s of analytical time. Fifty-eight elements were determined by spot-analysis and the spectra were converted by means of an average response factor K_Y into fully quantitative data as previously described (Gratuze, 2014). Reference materials Corning A and NIST 612 were repeatedly measured throughout the analytical run, and accuracy was within <5% for most major and minor elements and within 5–10% for minor and trace elements (Table S2).

Comparison of the EPMA and LA-ICP-MS results in relation to the recommended values for Corning A shows very good agreement for most

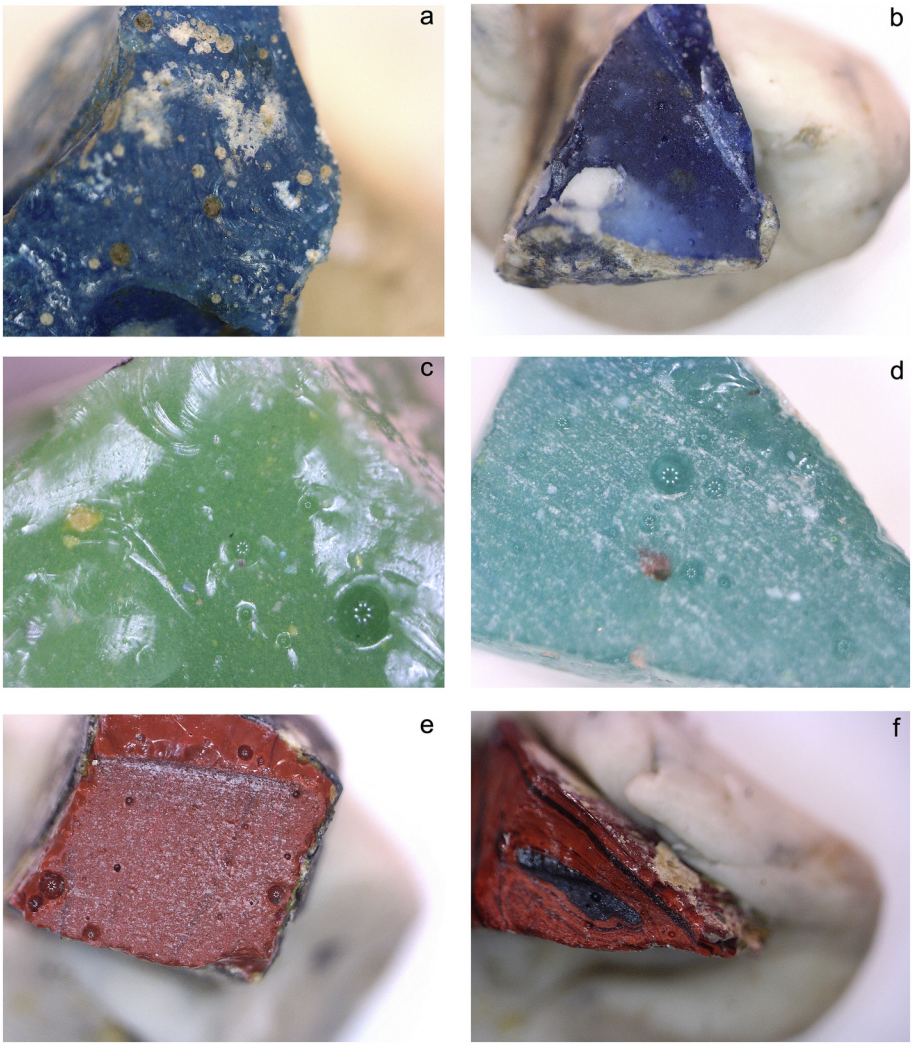

Fig. 4. Details of the surfaces of different tesserae under the optical microscope. (a) Bluish turquoise tessera KT NS 018; (b) cobalt blue tesserae KT NS 006; (c) green tessera KT NS 025; (d) blue green tessera KT NS 017; (e) homogeneous red tesserae KT NS 019; (f) stratified red ingot fragment KT NS 007. (For interpretation of the references to colour in this figure legend, the reader is referred to the web version of this article.)

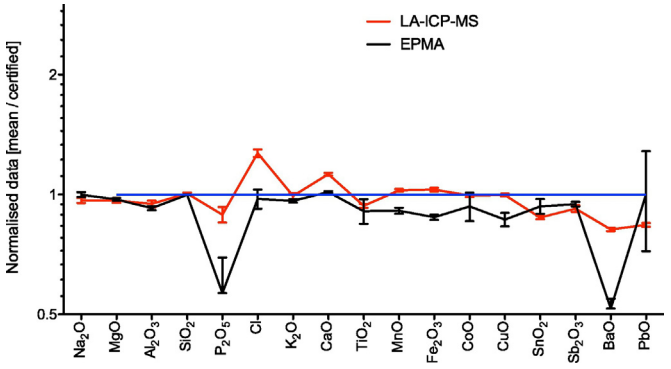

Fig. 5. Comparison of accuracy and precision of the LA-ICP-MS and EPMA analyses. The graph shows the averages of the Corning A glass standards normalised to the accepted reference values according to Vicenzi et al., 2002. Error bars indicate the relative standard deviation of the repeated measurements (n ≥ 9). The graph illustrates the extent of correspondence between the two analytical methods and between the analyses and the reference glass. The deviation from the reference values and the precision is generally better for the LA-ICP-MS data with the exception of lime, soda, lead and chlorine. Full data are given in Tables S1 and S2.

major and minor oxides with the given values as well as between the two analytical methods (Fig. 5). Overall, the LA-ICP-MS data corresponds closer to the recommended values than the EPMA results with the exception of lime, soda, lead and chlorine. However, the accuracy of the LA-ICP-MS calcium measurements increases significantly (better than 3%) when considering the NIST 612 standard that has higher calcium levels (Table S2). As regards the EPMA results, particularly the titanium, iron and manganese levels are somewhat problematic (approximately 10% deviation), and the LA-ICP-MS data was thus preferred.

2.3. SEM-EDS

The coloured tesserae were examined by SEM-EDS to investigate crystalline phases present in the glass matrix. The available equipment

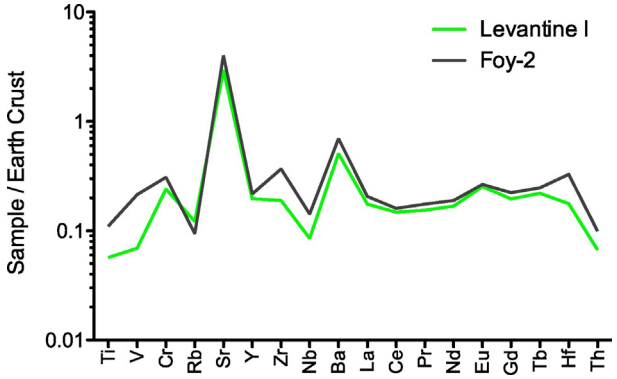

Fig. 7. Trace element patterns of the two identified glass groups. Averages are normalised to the mean values in the continental earth crust (Kamber et al., 2005).

used at IRAMAT-CEB was a FEI Philips XL40 ESEM with an Oxford Instrument EDX system for microanalysis (Link Pentafet Si(Li) detector). Imaging and analyses were done at 20 kV acceleration voltage, a beam diameter of 1 μm and at working distance of 10 mm. Semi-quantitative determination of the opacifiers and pigments was performed by X-ray microanalysis for 300 s time. The quantification was done using INCA software.

3. Results

3.1. Base glass characteristics

All the analysed samples can be classified as soda-lime-silica glass with low potassium and magnesium oxide contents (<1.5%), indicative of the use of mineral natron as fluxing agent typical of Roman and early medieval glassmaking prior to the ninth century CE (Table 1). Two different primary glass production groups can be identified based on the mineral components associated with the silica source such as

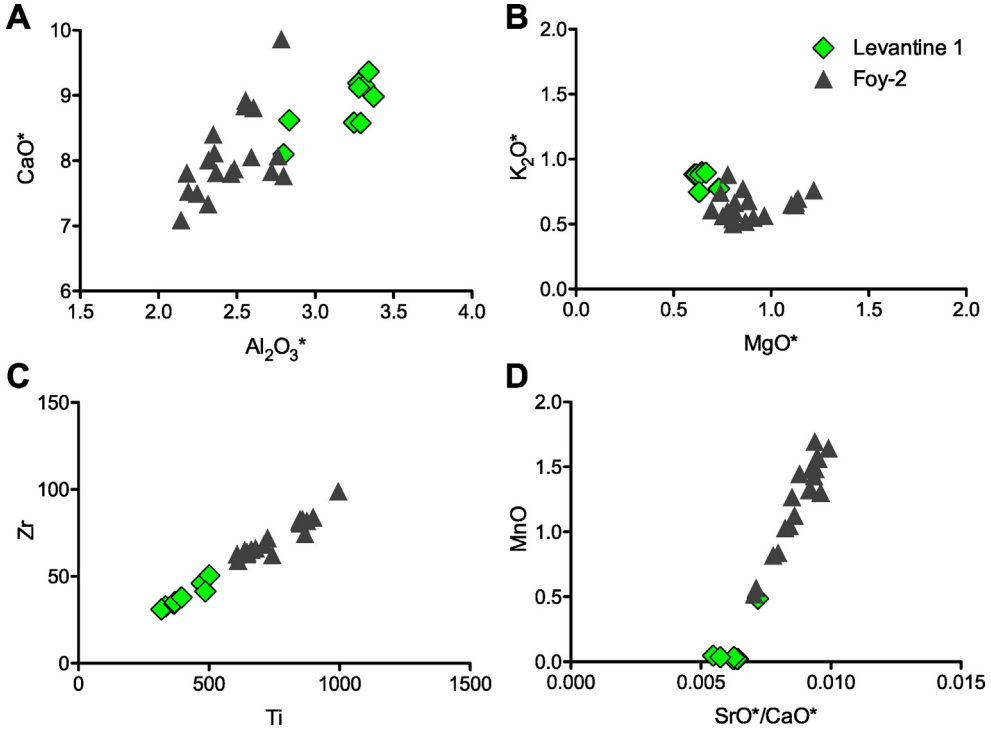

Fig. 6. Base glass composition of the Kilise Tepe samples. (a) Lime and alumina concentrations separate two groups, reflective of two different silica sources; (b) Potash and magnesia concentrations indicate the use of natron as fluxing agent; (c) Correlation between zirconium and titanium, while differences in the absolute values confirm the use of different silica sources; (d) Manganese and strontium to calcium ratios demonstrate that the manganese minerals of the Foy-2 group contribute strontium to the glass batch. Asterisks indicate reduced and normalised data.

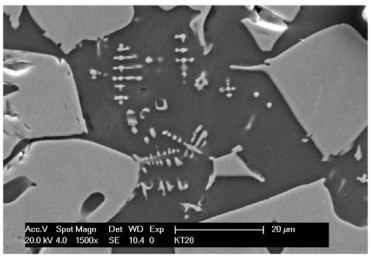

Fig. 8. SEM image of blue tesserae KT NS 028. Undissolved grains of cobalt oxide and crystals in the centre caused by devitrification (wollastonite).

aluminium, calcium, titanium and zirconium (Fig. 6). The largest compositional group (n = 19) is defined by elevated levels of magnesium, titanium and zirconium (Fig. 6b, c) and corresponds to the primary production group Foy-2, originally defined as série 2.1 by Foy et al. (2003; see also the definition in Schibille et al., 2016 a & b). This type of glass has variously been referred to as weak HIMT (Rosenow and Rehren, 2014), HIMT 2 (Conte and Chinni, 2014; Foster and Jackson, 2009), HLIMT (Ceglia et al., 2015) or CaO-rich HIMT (Gliozzo et al., 2016). This group has on average also higher strontium to calcium ratios, which are strongly correlated with manganese, providing evidence for the use of a source of manganese rich in strontium (Fig. 6d). The production and circulation of Foy-2 (série 2.1) is attested in the sixth and seventh centuries (Bonnerot et al., 2016; Ceglia et al., 2015; Cholakova et al., 2016; Conte and Chinni, 2014; Schibille et al., 2016a & 2016b), but manufacturing may have already begun in the fifth century (Foy et al., 2003). Judging from the compositional characteristics, the primary production location of this glass group is assumed to be in Egypt (Foy et al., 2003; Schibille et al., 2016a). The Foy-2 group encompasses all the red, yellow, black, blue and gold leaf tesserae as well as the gilded plaques and the vessel fragment (Table 1). The group of transparent gold glasses and vessel samples can be divided into two sub-groups, one that comprises tesserae KT NS 004 and KT NS 009 and the three gilded plaques with somewhat higher aluminium, calcium, magnesium, potassium, titanium, manganese and iron concentrations, the other group includes the remaining gold leaf tesserae and vessel fragment KT NS 008 (Table 1).

The remaining nine tesserae from Kilise Tepe show a typical Levantine I glass composition (Table 1), with high alumina and lime concentrations (Fig. 6a). Compared to the Foy-2 group, Levantine I glass has lower soda and magnesia contents and lower heavy element contaminations (Fe, Ti, Zr, V, Hf) (Table 1, Fig. 7). Levantine I glass was relatively widespread in the Mediterranean. It was produced in Syro-Palestine, for

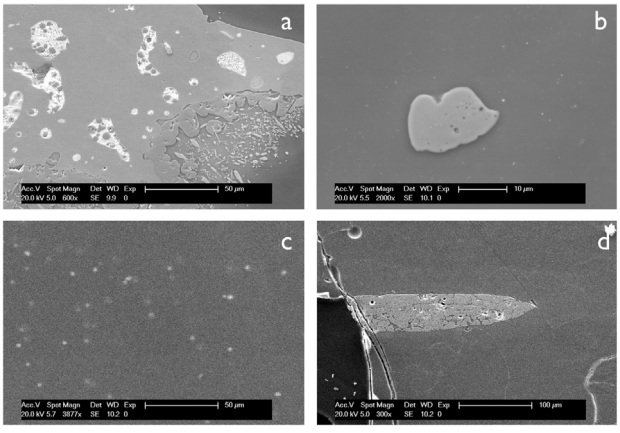

Fig. 9. SEM SE images of tesserae with metallic inclusions. (a) Lead-rich copper alloy particles in green tessera KT NS 025 partially dissolved (small particles on the right); (b) slightly rounded iron oxide particle in black tessera KT NS 016; (c) dispersed small metallic copper particles in red ingot KT NS 007; (d) inclusion of iron in sample KT NS 007.

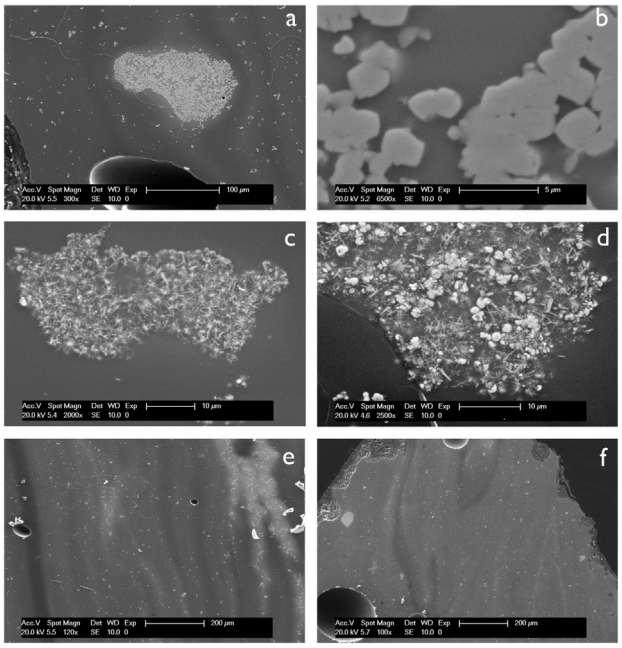

Fig. 10. SEM SE images of tesserae opacified with lead stannate. (a) Agglomeration of lead stannate particles in yellow tessera KT NS 014; (b) detail of amorphous crystals of the lead stannate cluster in KT NS 014; (c) cluster of partly melted amorphous crystals with needle-shaped crystals newly formed from the dissolution of the former in light green sample KT NS 001; (d) detail of the relationship between the amorphous and needle-shaped crystals; (e) light green tessera KT NS 001 showing streaks of concentrated lead stannate; (f) layering of lead rich phases with concentrated lead stannate in red tesserae KT NS 019.

instance, in the furnaces of Jalame in the fourth century (Brill, 1988; Freestone et al., 2000) and in Apollonia in the sixth century (Tal et al., 2004; Freestone et al., 2008). With the exception of one sample (KT NS 020) no significant amounts of manganese (typically < 300 ppm) was detected that would indicate its deliberate addition as colourant or decolourant (Fig. 6d). The low levels of manganese in the Levantine I tesserae from Kilise Tepe point to a sixth century date or later. Earlier Levantine glasses regularly contain elevated concentrations of manganese, such as the fourth-century assemblage at Jalame (Brill, 1988) or fifth-century Aquileia (Gallo et al., 2014), whereas the sixth- to seventh-century glasses from the primary production sites in Syria-Palestine (Freestone et al., 2000, 2008; Tal et al., 2004) do not typically contain added manganese. Interestingly, all the green and turquoise tesserae are of a Levantine I composition, plus the bluish aqua window glass fragment. A similar colour-specific trend was observed in relation to the turquoise and green tesserae from Hagios Polyeuktos in Constantinople (Schibille and McKenzie, 2014).

When comparing the rare earth element (REE) patterns, Foy-2 glasses tend to have on average higher values, especially for the heavy elements associated with iron and titanium such as vanadium and niobium, respectively (Fig. 7). However, even the lanthanides are slightly elevated in the Foy-2 samples compared to the Levantine I group. Taken together, this proves the use of different silica sources for the two glass groups and by extension, different geological and geographical origins.

3.2. Colour and opacity

Except for the seven gold leaf tesserae that exhibit only natural hues due to the iron oxide contained in the raw materials, all other tesserae are intensely coloured. The colour in glass can derive from the addition of transition metal ions dissolved in the glass, from metal nanoparticles in the glass (Cu), or from the dispersion of crystalline pigments in the matrix (Biron and Chopinet, 2013). In the Kilise Tepe samples, transition metal ions are used for blue (CoO) and turquoise (CuO) tesserae, metal

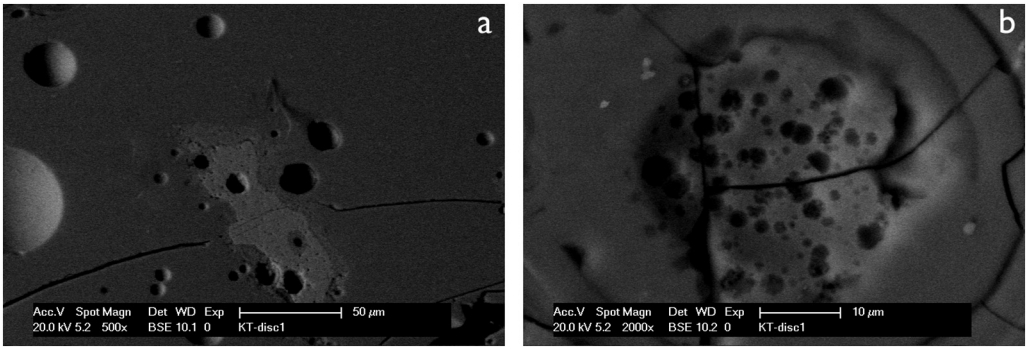

Fig. 11. SEM BSE images of tesserae KT NS 002. (a) Partially dissolved particle of calcium phosphate inclusion (lighter grey) surrounded by black gas bubbles; (b) gas bubbles in areas of higher phosphorus concentrations caused by the partially dissolved calcium phosphate particle.

particles in the black (Fe), green and red samples (Cu), while pigments of yellow stannate (Pb_2SnO_4) were detected in the yellow and green, as well as unexpectedly also in the red tesserae.

3.2.1. Cobalt and copper oxides as colourants

The dark blue tesserae contain cobalt as colourant that is associated with slightly elevated copper and iron concentrations. These elements were probably introduced unintentionally with the cobalt ore as shown in sample KT NS 028, where the undissolved sub-rectangular grains contain cobalt, iron and copper (Fe_2O_3 82%, CoO 16%, CuO 0.9%) (Fig. 8). The association with iron is consistent with the known Roman-type colourant of blue glass (Gratuze et al., 1992).

The different shades of green and turquoise tesserae have significant quantities of copper in the oxidized form (Table 1). Copper oxide brings about a light blue or turquoise colour. In the two turquoise tesserae the copper oxide is completely dissolved in the glass matrix, resulting in a translucent rather than an opaque quality. The opacification of sample KT NS 002 is caused by calcium phosphate particles (discussed below).

3.2.2. Metallic inclusions: Copper and iron

Some authors have hypothesised that by-products of metalworking were used for the colouration of glass (Mass et al., 1998; Freestone et al., 2003). The detection of metallurgical by-products in Roman glass is relatively rare (Wypyski and Becker, 2004), but it has been frequently attested in the late antique and Byzantine periods (Maltoni and Silvestri, 2016; Neri, 2016; Wypyski, 2005).

The Kilise Tepe tesserae provide clear evidence for this practice. Two green tesserae (KT NS 020 and 015) exhibit a combination of the yellow pigment lead stannate, and undissolved metallic particles in the glass matrix (Fig. 9a). Interestingly, these inclusions (50 μm–200 μm) correspond to a leaded copper alloy (Cu-Pb-Zn, 78.3%, 20.3%, 1.4%, respectively) that was used in late antique and Byzantine metallic objects (Ponting, 1999; Ashkenazi et al., 2015). The red tesserae are likewise

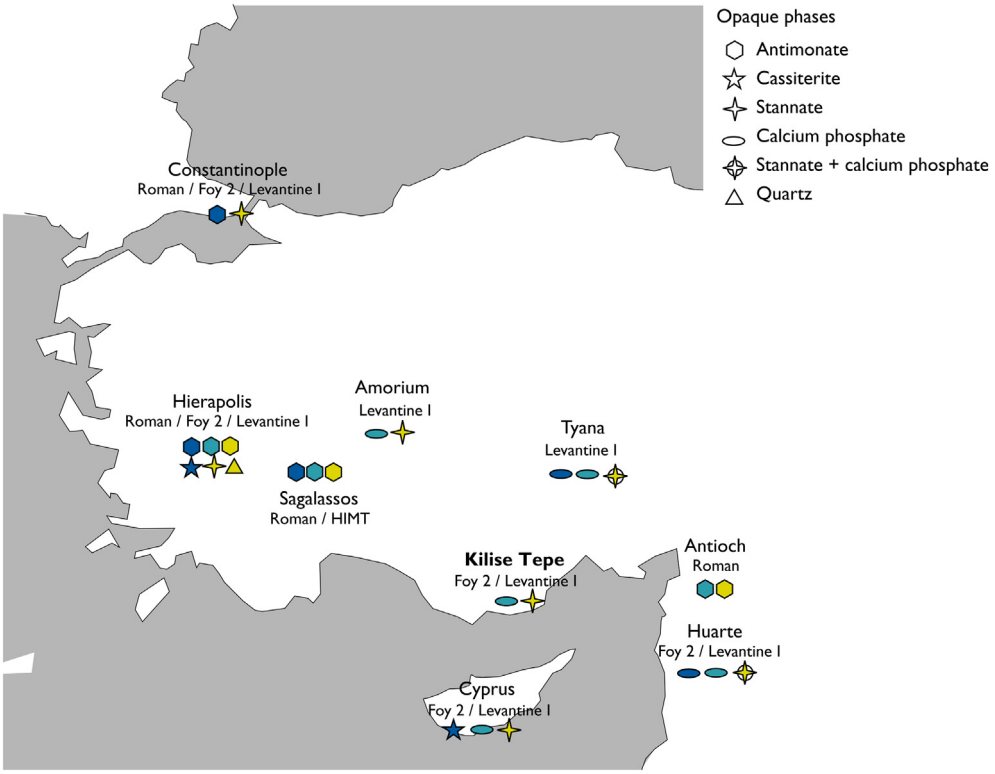

Fig. 12. Distribution of glass groups and opacifiers used for mosaic tesserae. Sixth-century mosaic assemblages (Amorium, Antioch, Constantinople, Cyprus, Hierapolis, Kilise Tepe and Tyana), and earlier fourth- to fifth-century material (Hierapolis, Huarte and Sagalassos). Data from Bonnerot et al., 2016; Lahanier, 1987; Neri et al., forthcoming; Schibille and McKenzie, 2014; Schibille et al., 2012; Silvestri et al., 2016; Wypyski, 2005; Wypyski and Becker, 2004.

Table 1
LA-ICP-MS data of the Kilise Tepe samples.
Major and minor oxides [wt%], including chlorine, and trace elements [ppm]. The crystalline phases have been stoichiometrically calculated based on semi-quantitative analyses by SEM-EDS.

	No	Context	Type	Colour	Opacity	Crystalline phases	Na_2O	MgO	Al_2O_3
Levantine I									
KT NS 001	J15/008	86,303	Tessera	Light green	Opaque	Lead stannate	13.28	0.49	2.65
KT NS 005	I14/252	75,316	Tessera	Blue green	Opaque		15.38	0.59	2.99
KT NS 015	M16/105	95,120	Tessera	Light green	Opaque	Lead stannate Metallic inclusions: Cu-Sn-Pb-Zn	13.11	0.49	2.61
KT NS 017	M16/074	95,104	Tessera	Blue green	Opaque	Lead stannate	15.56	0.59	3.03
KT NS 020	L16/006	93,201	Tessera	Dark green	Opaque	Metallic inclusions: Cu-Sn-Pb-Zn	15.09	0.62	2.40
KT NS 025	J15/014	86,307	Tessera	Green	Opaque	Lead stannate	15.37	0.58	3.00
KT NS 002	J15/008	86,303	Tessera	Light turquoise	Opaque	Calcium phosphate	16.74	0.71	2.72
KT NS 018	L18/160	93,102	Tessera	Bluish turquoise	Translucent		16.25	0.65	3.25
KT NS 021	M17/131	95,030	Window pane	Bluish aqua	Transparent		14.19	0.62	3.34
Foy-2									
KT NS 003	L18/006	73,000	Tessera	Red	Opaque	Lead stannate	17.65	0.79	2.24
KT NS 007	M18/326	78,801	Ingot	Red	Opaque	Lead stannate Metallic inclusion: Fe	16.21	0.77	2.25
KT NS 019	L16/036	93,212	Tessera	Red	Opaque	Lead stannate	17.18	0.81	2.27
KT NS 006	L16/006	93,201	Tessera	Blue	Translucent		17.95	0.76	2.67
KT NS 012	K15/118	95,402	Tessera	Blue	Translucent		18.46	0.73	2.75
KT NS 028	K15/028	86,414	Tessera	Blue	Translucent	Cobalt oxide: $CoO + Fe_2O_3$	18.74	0.68	2.54
KT NS 014	L16/011	93,200	Tessera	Yellow	Opaque	Lead stannate	17.83	0.72	2.07
KT NS 016	L16/027	93,211	Tessera	Black	Translucent	Metallic inclusions: Fe-Mn	18.15	0.79	2.29
KT NS 010	L17/039	93,303	Gold tessera	Amber tinge	Transparent		18.79	0.89	2.30
KT NS 011	L17/006	93,302	Gold tessera	Amber tinge	Transparent		18.49	0.94	2.29
KT NS 013	L17/013	93,302	Gold tessera	Amber tinge	Transparent		18.45	0.76	2.19
KT NS 026	J15/012	86,306	Gold tessera	Amber tinge	Transparent		18.26	0.73	2.14
KT NS 027	J15/14	86,307	Gold tessera	Amber tinge	Transparent		18.79	0.78	2.09
KT NS 008	M17/181	95,005	Bowl base	Amber tinge	Transparent		19.63	0.85	2.13
KT NS 004	K15/023	86,409	Gold tessera	Greenish tinge	Transparent		17.62	1.11	2.71
KT NS 009	M16/111	95,124	Gold tessera	Greenish tinge	Transparent		18.19	1.09	2.53
KT NS 022	K15/111	95,400	Gold plaque	Greenish tinge	Transparent		20.09	1.18	2.68
KT NS 023	L18/164	93,102	Gold plaque	Greenish tinge	Transparent		17.88	1.08	2.49
KT NS 024	L18/160	93,102	Gold plaque	Greenish tinge	Transparent		17.85	1.10	2.49

	Li	B	Ti	V	Cr	Co	Ni	Zn	Ga	As	Rb	Sr	Y	Zr	Nb	Mo	Ag	Cd	Sb	Cs	Ba
Levantine I																					
KT NS 001	3.10	90	333	6.42	13.18	2.66	20.36	32.24	3.05	21.08	9.28	371	5.70	32.80	1.13	0.63	39.04	0.07	99.84	0.10	180
KT NS 005	3.70	97	371	7.42	14.38	2.41	22.92	29.79	3.54	17.06	10.58	456	6.71	35.07	1.30	0.80	13.65	0.03	20.22	0.09	205
KT NS 015	3.26	88	318	6.15	11.08	2.75	20.82	31.80	3.02	23.03	8.97	358	5.47	31.02	1.10	0.64	50.27	0.12	107.14	0.10	175
KT NS 017	4.07	100	366	7.43	14.39	2.50	23.25	29.59	3.49	18.46	10.50	453	6.52	34.30	1.29	0.77	13.74	0.04	22.58	0.10	200
KT NS 020	4.93	117	472	14.05	15.43	10.20	32.86	134	3.39	95	8.49	445	5.99	46.04	1.48	1.24	23.83	0.12	219.55	0.12	231
KT NS 025	3.55	100	368	7.37	13.74	2.45	22.60	29.75	3.70	18.49	10.41	451	6.66	35.08	1.28	0.80	13.74	0.06	20.11	0.09	201
KT NS 002	3.83	130	501	9.31	26.03	2.97	17.09	26.48	3.16	10.46	8.67	364	6.01	50.50	1.51	0.80	6.40	0.00	3.94	0.08	181
KT NS 018	4.35	109	395	7.94	15.71	6.06	17.16	31.75	3.69	15.95	10.93	483	6.90	37.95	1.31	0.78	12.86	0.03	7.32	0.10	214
KT NS 021	4.56	81	486	10.50	18.46	2.16	6.09	11.03	3.73	1.59	9.67	432	6.97	41.44	1.54	0.44	0.16	0.03	1.21	0.10	244
Foy-2																					
KT NS 003	6.05	145	678	23.33	18.85	7.39	21.90	59.55	3.77	11.01	7.39	563	6.53	66.14	2.07	1.85	5.48	0.05	80.43	0.13	247
KT NS 007	4.65	125	743	23.11	18.82	172	143.46	2721	4.09	135	7.27	481	6.41	62.18	2.01	2.45	4.33	0.01	208.62	0.09	237
KT NS 019	5.49	146	868	26.08	23.50	137	99.23	1719	4.20	97	7.03	501	6.64	74.44	2.21	2.25	5.37	0.04	253.94	0.11	442
KT NS 006	4.44	136	898	22.03	29.52	461	32.35	24.91	4.42	1.75	9.47	462	7.07	84.10	2.21	2.68	0.53	0.04	4.45	0.09	242
KT NS 012	4.72	141	876	20.24	25.67	247	19.91	19.48	4.16	2.31	8.78	455	6.90	81.97	2.08	1.81	0.43	0.04	1.53	0.08	228
KT NS 028	4.82	134	612	23.28	16.82	489	19.80	27.71	6.85	3.35	7.78	519	6.65	59.05	1.79	3.91	0.55	0.07	5.29	0.12	289
KT NS 014	5.14	153	638	24.57	14.37	5.46	11.65	23.04	3.93	110	6.24	509	6.28	63.58	1.84	2.14	21.95	0.08	166.36	0.06	279
KT NS 016	6.65	148	644	22.53	17.14	15.09	12.43	27.23	3.75	13.50	8.17	538	6.48	63.02	1.93	1.80	3.40	0.05	72.52	0.14	252
KT NS 010	5.40	163	725	23.43	18.54	6.23	9.15	23.56	4.14	3.11	6.76	570	6.84	72.09	2.13	1.80	0.44	0.02	188.96	0.08	228
KT NS 011	5.88	222	711	25.79	17.17	7.80	9.68	22.20	4.15	2.93	6.44	638	6.77	68.46	2.17	1.75	0.37	0.04	67.15	0.06	234
KT NS 013	5.48	196	646	25.16	14.22	5.35	9.58	17.75	3.98	1.89	6.74	571	6.35	63.89	1.95	2.81	0.29		4.71	0.06	275
KT NS 026	5.62	189	662	24.82	17.36	5.31	9.42	17.99	4.21	2.76	6.75	580	6.55	65.48	1.98	2.73	0.24	0.05	7.27	0.08	277
KT NS 027	4.89	185	637	26.23	16.28	5.37	9.33	14.79	4.07	2.91	6.03	562	6.64	64.93	1.96	1.78	0.33	0.06	20.43	0.07	279
KT NS 008	5.08	167	608	22.61	15.71	4.18	7.67	12.03	3.75	2.14	6.52	566	6.36	62.77	1.85	2.02	0.23	0.05	10.50	0.08	230
KT NS 004	8.25	192	996	30.56	24.91	6.70	11.48	22.78	4.79	1.86	8.63	773	8.20	98.90	3.10	1.66	0.59	0.05	150.95	0.12	260
KT NS 009	7.46	167	849	33.00	20.81	10.65	12.91	25.04	4.92	10.32	7.57	679	7.50	80.61	2.46	2.88	1.42	0.05	87.59	0.16	319
KT NS 022	8.53	187	849	31.67	18.93	8.52	16.84	22.12	4.97	4.93	7.44	657	7.71	82.84	2.61	4.09	0.33	0.09	142.70	0.11	356
KT NS 023	7.26	162	847	30.66	20.00	9.20	11.95	23.67	4.60	3.90	7.46	685	7.59	81.72	2.54	2.49	0.43	0.06	82.90	0.11	297
KT NS 024	7.22	162	858	32.08	20.56	9.67	12.27	24.54	4.97	4.16	7.81	696	7.77	82.91	2.54	2.66	0.79	0.08	88.29	0.10	310

SiO_2	P_2O_5	Cl	K_2O	CaO	MnO	Fe_2O_3	PbO	CuO	SnO_2
Levantine I									
56.97	0.09	0.87	0.72	7.00	0.02	0.33	14.20	0.96	2.16
62.69	0.08	0.96	0.82	8.39	0.02	0.37	5.37	1.38	0.75
55.12	0.08	0.84	0.70	6.80	0.02	0.33	16.36	0.95	2.35
62.58	0.08	0.97	0.82	8.37	0.02	0.37	5.22	1.40	0.80
58.03	0.25	0.81	0.65	7.31	0.49	0.56	10.23	1.96	1.29
62.93	0.08	1.00	0.81	8.35	0.02	0.38	5.17	1.39	0.72
67.83	0.46	0.86	0.75	7.87	0.05	0.45	0.08	1.20	0.06
66.57	0.11	0.97	0.87	9.10	0.04	0.40	0.14	1.33	0.09
70.44	0.11	0.90	0.74	8.88	0.04	0.53	0.001	0.001	0.0001
Foy-2									
62.69	0.17	0.79	0.57	7.75	1.13	4.80	0.094	0.98	0.06
59.67	0.47	0.80	0.70	7.13	0.84	3.62	3.63	1.21	1.98
60.75	0.43	0.83	0.62	7.19	1.03	3.08	2.59	0.82	1.78
66.79	0.19	0.92	0.86	7.68	0.57	1.15	0.023	0.053	0.0014
66.76	0.16	0.97	0.73	7.63	0.52	0.91	0.015	0.039	0.0010
66.19	0.14	0.88	0.60	7.89	0.82	1.11	0.010	0.082	0.0017
60.96	0.04	0.86	0.48	6.56	1.32	0.68	7.37	0.019	0.76
63.50	0.10	0.83	0.64	7.57	1.05	3.72	0.86	0.12	0.09
66.26	0.07	0.85	0.54	7.92	1.27	0.75	0.038	0.009	0.0039
66.14	0.07	0.82	0.55	8.20	1.33	0.80	0.024	0.008	0.0025
67.31	0.06	0.86	0.58	7.31	1.48	0.70	0.004	0.004	0.0008
67.64	0.05	0.88	0.55	7.34	1.43	0.68	0.004	0.004	0.0008
67.68	0.05	0.91	0.49	6.92	1.30	0.67	0.002	0.003	0.0004
65.92	0.06	0.93	0.50	7.61	1.45	0.64	0.001	0.003	0.0002
64.35	0.09	0.81	0.68	9.61	1.56	1.04	0.008	0.006	0.0017
64.85	0.12	0.85	0.65	8.56	1.70	1.05	0.035	0.011	0.0019
63.32	0.12	0.95	0.74	7.84	1.65	1.04	0.006	0.007	0.0006
65.53	0.11	0.79	0.63	8.62	1.48	1.01	0.025	0.009	0.0017
65.32	0.11	0.80	0.63	8.69	1.58	1.04	0.029	0.010	0.0018

La	Ce	Pr	Nd	Sm	Eu	Gd	Tb	Dy	Ho	Er	Tm	Yb	Lu	Hf	Ta	W	Pt	Au	Bi	Th	U
Levantine I																					
5.25	9.66	1.19	5.11	1.04	0.38	1.11	0.21	0.95	0.20	0.59	0.074	0.51	0.072	0.83	0.067	0.060	0.0050	0.16	546	0.68	0.43
6.08	11.49	1.38	5.97	1.20	0.44	1.26	0.24	1.06	0.22	0.70	0.083	0.55	0.084	0.87	0.074	0.069	0.0070	0.26	8.87	0.74	0.51
4.86	9.10	1.15	4.78	1.01	0.35	1.13	0.19	0.90	0.19	0.56	0.071	0.51	0.070	0.81	0.066	0.057	0.0030	0.20	613	0.64	0.43
5.73	10.76	1.35	5.63	1.18	0.42	1.32	0.23	1.03	0.23	0.65	0.082	0.57	0.081	0.84	0.077	0.065	0.0010	0.28	8.86	0.72	0.50
5.54	9.73	1.26	5.34	1.11	0.38	1.25	0.21	0.95	0.21	0.60	0.084	0.54	0.081	1.14	0.090	0.709	0.0038	0.33	105	0.82	0.79
5.98	11.12	1.40	5.88	1.21	0.40	1.27	0.22	1.02	0.23	0.65	0.084	0.55	0.077	0.88	0.078	0.074	0.0030	0.30	8.70	0.73	0.49
5.81	10.38	1.29	5.46	1.12	0.37	1.18	0.21	0.97	0.21	0.64	0.075	0.55	0.083	1.22	0.082	0.061	0.0037	0.20	0.77	0.84	0.59
6.10	11.34	1.40	5.97	1.25	0.44	1.42	0.24	1.08	0.23	0.69	0.088	0.61	0.088	0.94	0.082	0.069	0.0024	0.31	0.87	0.75	0.51
6.39	11.73	1.44	6.23	1.24	0.45	1.42	0.23	1.11	0.23	0.69	0.087	0.62	0.088	1.06	0.086	0.058	0.0012	nd	0.01	0.85	0.79
Foy-2																					
6.66	11.42	1.45	5.99	1.22	0.41	1.29	0.24	1.12	0.23	0.71	0.090	0.62	0.094	1.67	0.12	0.15	0.0046	0.14	0.60	1.09	1.27
6.34	10.69	1.36	5.75	1.16	0.39	1.20	0.23	1.07	0.22	0.64	0.086	0.60	0.091	1.52	0.12	0.25	0.0037	0.01	9.16	1.02	1.07
6.37	10.82	1.44	5.95	1.23	0.44	1.40	0.24	1.13	0.24	0.71	0.093	0.68	0.098	1.79	0.13	0.32	0.0039	0.19	7.52	1.08	1.12
6.99	12.33	1.55	6.48	1.29	0.44	1.34	0.26	1.15	0.25	0.75	0.095	0.67	0.097	1.96	0.13	0.15	0.0037	nd	0.012	1.13	1.03
6.35	11.25	1.45	6.07	1.30	0.42	1.45	0.24	1.16	0.25	0.73	0.093	0.67	0.100	1.98	0.12	0.13	0.0052	0.018	0.010	1.03	0.99
6.40	10.98	1.43	5.89	1.19	0.40	1.28	0.22	1.08	0.22	0.69	0.092	0.62	0.092	1.43	0.10	0.26	0.0032	0.11	0.024	0.99	1.18
6.06	9.75	1.31	5.47	1.21	0.37	1.34	0.21	1.07	0.22	0.66	0.090	0.62	0.089	1.49	0.11	0.32	0.0031	0.074	11.14	0.95	1.17
6.25	10.54	1.37	5.71	1.18	0.39	1.36	0.23	1.09	0.24	0.69	0.087	0.58	0.094	1.49	0.12	0.20	0.0037	0.047	13.97	1.01	1.15
6.48	11.07	1.44	6.15	1.27	0.40	1.50	0.25	1.16	0.24	0.71	0.089	0.69	0.104	1.73	0.13	0.14	0.0061	0.020	0.029	1.08	1.18
6.50	10.97	1.47	6.20	1.29	0.41	1.53	0.25	1.11	0.24	0.76	0.094	0.68	0.096	1.73	0.12	0.11	0.0040	0.014	0.045	1.06	1.46
5.98	10.07	1.33	5.66	1.19	0.37	1.38	0.22	1.04	0.23	0.67	0.083	0.65	0.089	1.49	0.11	0.16	0.0044	0.020	0.025	0.94	1.28
6.33	10.52	1.39	5.93	1.22	0.39	1.28	0.22	1.09	0.23	0.67	0.084	0.62	0.10	1.52	0.11	0.17	0.00048	0.008	0.027	1.01	1.25
6.65	10.93	1.45	6.07	1.18	0.38	1.32	0.23	1.15	0.22	0.69	0.088	0.67	0.090	1.55	0.11	0.16	0.0012	0.0043	0.014	1.00	1.32
6.01	10.30	1.35	5.76	1.16	0.38	1.38	0.21	1.05	0.22	0.69	0.090	0.62	0.086	1.55	0.11	0.16	0.0026	0.0025	0.0088	1.00	1.06
8.30	14.25	1.80	7.66	1.64	0.46	1.63	0.30	1.38	0.28	0.89	0.11	0.82	0.12	2.34	0.19	0.16	0.0058	nd	0.017	1.50	1.53
7.14	11.74	1.59	6.94	1.48	0.46	1.67	0.26	1.26	0.26	0.79	0.10	0.76	0.11	1.91	0.14	0.23	0.0040	0.039	0.047	1.23	1.20
7.37	12.54	1.64	6.97	1.46	0.48	1.59	0.27	1.31	0.27	0.81	0.12	0.76	0.11	1.95	0.16	0.24	0.0046	0.0022	0.024	1.27	1.09
7.40	12.50	1.65	6.85	1.47	0.43	1.52	0.27	1.31	0.27	0.80	0.10	0.73	0.10	2.01	0.15	0.18	0.0041	0.0094	0.045	1.29	1.29
7.52	12.64	1.69	6.93	1.46	0.45	1.58	0.27	1.25	0.27	0.80	0.10	0.73	0.11	1.96	0.14	0.20	0.0039	0.0066	0.051	1.27	1.25

coloured by a copper compound. Judging from the associated elements and comparative materials, copper is present presumably in the form of nanoparticles of metallic copper (Fig. 9b). In the ingot fragment (KT NS 007) and one of the tesserae (KT NS 019), copper is linked to increased tin and zinc contents suggesting the use of a metallurgical by-product as shown in previous studies (Barber et al., 2009; Freestone, 1987; Freestone et al., 2003; Nakai et al., 1999; Santagostino Barbone et al., 2008).

The production of red tesserae is technically demanding, and requires a strongly reducing atmosphere and/or the addition of reducing agents. Partial re-oxidation or incomplete reduction of the copper can render red glass a darker red (Freestone et al., 2003). The iron present in high quantities (2.5–3.8%) suggests its intentional use, maybe to help reduce the cuprous ions to metallic copper. In fact, an inclusion of iron oxide (with traces of manganese and titanium) was detected in the ingot (Fig. 9d). Tin can have similar reducing effects (Freestone et al., 2003). One of the tesserae (KT NS 003) as well as the ingot (KT NS 007) exhibit opaque dark red streaks alternated with transparent green ones (Fig. 4f). The chemical composition of the red and transparent green streaks is similar, because in the latter, the pigment has simply dissolved and the copper ion determines the dark green colour (Wypyski and Becker, 2004; Neri et al., 2013).

The black tessera is translucent, it is black with a shade of green rather than purple or blue, which is probably produced by a combination of a large amount of iron and reducing conditions (Wypyski and Becker, 2004; Biron and Chopinet, 2013). Copper and lead are also slightly elevated, probably as a result of the use of a copper alloy, that in the reduced form can form metallic droplets. The SEM image clearly shows the large grey inclusion of metallic iron and small round crystals of metallic copper (Fig. 9b).

3.2.3. Pigments: Lead stannate

The high amount of lead and tin in the green tesserae and in two red samples (KT NS 019 and 07) is caused by the introduction of yellow pigments that consist mainly of lead and tin (PbO 35–60%; SnO_2 28–49%), in addition to silica (SiO_2 around 7%) and iron (Fe_2O_3 1.4%). This composition corresponds to yellow lead stannate crystals that are either slightly rounded squares (2.5 μm) aggregated in clusters (10 μm–200 μm) (Fig. 10a, b), or minute needle-like crystals dispersed in the matrix or again aggregated in clusters (10 μm–150 μm) (Fig. 10c). In some cases, these needle-like crystals are associated with round crystals and appear to be newly formed from the dissolution of the latter (Fig. 10d). These crystals generate a yellow colour and tend to be more concentrated in the light green tesserae than in the blue green ones (Table 1). They are arranged in layers (Fig. 10 e, f), because lead stannate was probably added to the molten glass as a pre-formed pigment similar to what is known about the use of lead antimonate, called *anime*. To avoid dissolution of the pigment, it would have been stirred in quickly and immediately poured into slabs (Moretti and Hreglich, 1984; Lahlil et al., 2008; Neri, 2016). Yellow lead stannates are often considered typical of Byzantine tesserae, in contrast to the Roman tradition where lead antimonate was commonly used. Recent studies have shown, however, that lead stannates occasionally appear already in yellow glasses of the Roman period (Verità et al., 2013).

3.2.4. Calcium phosphate

One light turquoise tessera (KT NS 002) has many voids and air bubbles and exceptionally high phosphorus contents that are evident in some of the individual EPMA area measurements (not shown). Small white patches (2–4 μm) high in calcium and phosphorus point to the use of calcium phosphate possibly in the form of bone ash (Fig. 11). The addition of calcium phosphate to a glass melt generates bubbles as well as a crystalline phase, due to devitrification processes, thus causing opacification (Silvestri et al., 2016). The use of this type of opacification is attested in turquoise, blue and green tesserae from the fifth century on, and seems to replace antimony-based opacifiers used until the fourth century CE (Turner and Rooksby, 1959; Lahlil et al., 2008; Lahlil et al., 2009; Silvestri et al., 2012). It is a peculiar technique, widespread above all in the Levantine area (Syria, Jordan, Cyprus, southern and central Turkey: Lahanier, 1987; Marii, 2013; Lachin et al., 2009; Wypyski, 2005; Bonnerot et al., 2016) and in some rare cases in northern Italy (Ravenna, Milan, Padua: Verità, 2010; Neri, 2016; Silvestri et al., 2012, 2016), where it was probably imported from the Levant by the Adriatic route.

4. Discussion

4.1. Kilise Tepe tesserae

Although the re-use of older mosaics from the dismantling of ancient buildings is a common phenomenon during late antiquity (e.g. Freestone, 1993; Freestone et al., 1990; DeLaine, 1997; Greenhalgh, 1989; Cutler, 2002; François and Spieser, 2002; Freestone, 2015), the tesserae of Kilise Tepe have evidently been produced from new, imported raw materials, rather than being recycled. Both the raw glass types as well as the opacification with calcium phosphate can generally be attributed to the fifth century or later and thus strongly suggest that the tesserae were newly produced for the decoration campaign of the early Byzantine church at Kilise Tepe.

The presence of undissolved colourants, like yellow pigments and metallic inclusions, proves that the glasses were coloured with additives and not through a simple mixture of coloured glass (Freestone, 1993; Gratuze et al., 1992). For example, the light turquoise tessera bears witness to a particular opacification technique using calcium phosphate. The green and yellow tesserae were coloured by adding lead stannate under oxidizing conditions, whereas the black and the red tesserae were coloured by metallic inclusions in a reducing atmosphere. The wide range of different colouration and opacification techniques possibly reflect the output of different secondary workshops, making a local production of the different tesserae most unlikely.

The colouring and opacifying technologies in the Kilise Tepe assemblage do not necessarily correspond to differences in the base glass composition. On the contrary, while the green tesserae are made from Levantine I glass, the base glass of the yellow tessera is of the Foy-2 type despite using the same or at least similar yellow lead stannate compound as colouring and opacifying agent. Generally, however, tesserae of the same colour were produced from the same primary glass at Kilise Tepe. This may imply secondary workshops that specialised in the production of a single colour and that received supplies from one primary production centre alone. Similar observations have been made in connection with the late antique mosaics from Sagalassos and Padua (Schibille et al., 2012; Silvestri et al., 2014) and as regards specific colours such as red (Freestone et al., 2003; Barber et al., 2009), flesh tones (Verità and Santopadre, 2010), yellow (Verità et al., 2013), and blue (Gratuze et al., 1992), as well as gold leaf tesserae (Neri and Verità, 2013; Neri et al., 2016).

The gold leaf tesserae from Kilise Tepe are somewhat exceptional in that they can be divided into two compositional sub-groups of the Foy-2 type (Table 1). One group comprises most of the gold leaf tesserae as well as the vessel fragment (samples KT NS 010, 011, 013, 026, 027 and 008), demonstrating that the glass used for tesserae production was the same as the glass employed for other artefacts. The other group consists in only two gold leaf tesserae and the three gilded plaques (samples KT NS 004, 009, 022, 023 and 024). The two groups differ in terms of their magnesium, aluminium, calcium, titanium and iron concentrations. These differences imply that workshops specialising in the production of gold leaf tesserae acquired their raw material from more than one primary producer. It has previously been demonstrated that the same secondary workshops (above all in the Levantine area) used different raw glasses for the production of gold leaf tesserae with different optical properties (Neri et al., 2016). The samples of the two different groups from Kilise Tepe indeed express slightly

different shades as the higher iron contents of the second group shifts the colour towards green. The difference is not very pronounced and cannot unequivocally be ascribed to aesthetic choices. However, the chemical data confirm our previous assumption that at least some of the gold leaf tesserae could have been cut from the larger gilded plaques found at Kilise Tepe.

In general, the main type of glass used in the production of the Kilise Tepe tesserae was the Foy-2 glass group with a likely provenance in Egypt. Levantine I was used for only a third of the analysed samples and it is associated with a specific range of colours, namely green and turquoise as well as the bluish aqua window glass fragment. Similar colour-specific trends have been noted as regards the late antique tesserae from the church of Hagios Polyeuktos in Constantinople (Schibille and McKenzie, 2014). What was then designated as the low manganese group (equivalent to Levantine I), comprises likewise only different shades of green and turquoise. All other samples from Hagios Polyeuktos correspond more closely to the Foy-2 type glass. These shared characteristics in terms of base glass to colour relationship further substantiate a production model whereby secondary workshops specialised in the manufacture of a limited colour range.

4.2. Mosaic tesserae from Asia Minor

The Kilise Tepe assemblage fits the overall pattern in the use of mosaic tesserae in Asia Minor and related areas that relied on imports from Egypt and the Levante (Fig. 12). Egyptian glasses (HIMT, Foy-2) were identified among the mosaic assemblages from Amorium, Antioch, Huarte, Cyprus, Hagios Polyeuktos and Hierapolis (Wypyski and Becker, 2004; Lahanier, 1987; Bonnerot et al., 2016; Schibille and McKenzie, 2014). As far as can be deduced from the published SEM-EDS data, Foy-2 glass seems to have been used for most of the manganese-containing tesserae from Cyprus (Bonnerot et al., 2016). Levantine glass makes up the majority of the tesserae from Huarte, Antioch, Tyana and Hierapolis (Lahanier, 1987; Wypyski and Becker, 2004; Wypyski, 2005; Lachin et al., 2009; Neri et al., forthcoming). The tesserae from Sagalassos are of a Levantine origin, but with some high titanium samples particularly among dark blue and red tesserae from the Apollo Klarios Temple (Schibille et al., 2012).

The Kilise Tepe tesserae differ from earlier Roman tesserae both in terms of the base glass as well as the opacification technologies. Roman tesserae are usually produced from a raw glass originating on the Levantine coast and opacified by calcium antimonate (Wypyski and Becker, 2004). For example, in fourth-century Antioch, late Roman Sagalassos, sixth-century Constantinople (blue tesserae) and in the church of the theatre of Hierapolis the majority of tesserae are opacified by antimony-based compounds, according to the Roman tradition. The tesserae from all other sites in Asia Minor for which data are available (Amorium, Tyana, Hierapolis, Huarte, Constantinople and Cyprus) testify to new opacification techniques that we also detected at Kilise Tepe. Bone ash appears mostly among mosaic assemblages from the south-eastern part of Asia Minor, Cyprus and Jordan starting in the fifth century CE (Werner and Bismon, 1967; Lahanier, 1987; Newton and Davison, 1999; Marii and Rehren, 2009). This confirms what has been noted elsewhere, namely that antimony-based opacifiers, used from about 1500 BCE to the fourth century CE, were gradually replaced by alternatives during the fifth to sixth centuries CE (Turner and Rooksby, 1959; Uboldi and Verità, 2003; Tite et al., 2008; Gratuze, 2012; Neri et al., 2013). Nonetheless, antimony continues to be used as an opacifier, most notably in the imperial capitals, in Constantinople until the sixth century (Schibille and McKenzie, 2014) and in Ravenna and Rome until the medieval period (Verità, in press). Generally, antimony appears to have been more widely employed in the production of tesserae in the western Mediterranean and Italy (Silvestri et al., 2011; Neri and Verità, 2013; Neri et al., 2016).

4.3. Workshop practices and supply

The variations in the opacification technique imply different secondary workshop traditions. Firstly, a uniform technique with antimony-based opacifiers and a typical late Roman base glass of Levantine origin, as identified in the blue, green, turquoise and yellow tesserae from Antioch, Sagalassos and Hierapolis (church of the theatre). From the sixth century on, tesserae exhibited a greater variety both in terms of the base glass as well as the opacification techniques. This change is documented, for instance, in the sixth-century mosaic tesserae from Constantinople, Cyprus, Hierapolis (St. Philip), Amorium and Kilise Tepe, providing clear evidence for a certain degree of diversification in the production of mosaic tesserae and consequently a multiplication of suppliers.

The comparison of the Kilise Tepe data with other recent analytical studies for Byzantine mosaic tesserae from the eastern Mediterranean (Moropoulou et al., 2016; Schibille and McKenzie, 2014; Schibille et al., 2012; Wypyski, 2005; Bonnerot et al., 2016; Lahanier, 1987; Lachin et al., 2009; Silvestri et al., 2016; Wypyski and Becker, 2004) highlights some geographical affinities of the opacification techniques and raw materials (Fig. 12). Blue tesserae produced with Foy-2 glass and coloured with an iron-rich cobalt source were found in Cyprus, Antioch, Sagalassos and Constantinople. Light blue or turquoise tesserae, containing copper or cobalt as colourant and calcium phosphate (Ca_3PO_4) as opacifier in a Levantine I glass matrix were identified in Huarte, Tyana, Amorium and Cyprus (Lahanier, 1987; Lachin et al., 2009; Silvestri et al., 2016; Wypyski, 2005; Bonnerot et al., 2016). Lead-tin opacification was detected in the green and yellow tesserae from Amorium, Constantinople, Cyprus and Hierapolis (Moropoulou et al., 2016; Schibille and McKenzie, 2014; Wypyski, 2005; Bonnerot et al., 2016; Neri et al., forthcoming). Interestingly, the lead-tin opacified samples can be either of a Levantine I or a Foy-2 base glass, depending on the colour. Green seems to be predominantly made of Levantine I, while the yellow samples correspond instead to the Foy-2 primary production group.

The production of red and black tesserae does not vary significantly from the Bronze age to the Byzantine period (Freestone et al., 2003; Barber et al., 2009; Wypyski and Becker, 2004). However, from the sixth century on some differences can be seen in the metallurgical by-product used (Fiori et al., 2004; Freestone et al., 2003; Gliozzo et al., 2012, Santagostino Barbone et al., 2008; Shugar, 2000; Verità et al., 2008). At Kilise Tepe and Hierapolis, iron and lead stannate was added to obtain a brown hue and/or to act as reducing agents. This has not previously been observed. Substantial amounts of either manganese, as in Constantinople and Amorium, or iron as in Kilise Tepe and Antioch were employed to produce black tesserae.

5. Conclusion

The close similarities between the tesserae from Kilise Tepe and those of other roughly contemporary sites in south-western Asia Minor, Cyprus and northern Syria appear to indicate that the different sites were part of a well-established supply network. The variability of the raw glass and secondary working techniques identified among the Kilise Tepe samples in comparison to other assemblages shed further light on the chronological developments of tesserae production. The raw glasses employed (Foy-2, Levantine I) circulated during the early Byzantine period, and most likely post-date the fifth century CE. Concurrent with a fifth-century date is also the tradition of using calcium phosphate as opacifier. This seems to confirm a late antique date for the mosaic tesserae. Technically, all the samples investigated here could have been part of the same mosaic programme, no repairs or restoration from later periods are evident. The multiplicity of production techniques marks a diversification in the supply, a phenomenon that is also observed in other eastern Mediterranean sites. Our data thus add to the mounting evidence indicating the multiplication of

secondary workshops for the production of glass tesserae during the fifth or sixth century CE and a modification of the more centralized Roman glass working tradition. This is reflected, in both, the variability of the raw glass as well as the colouring and opacifying agents found at a single site.

Supplementary data to this article can be found online at http://dx.doi.org/10.1016/j.jasrep.2016.12.036.

Acknowledgements

We thank the Turkish Ministry of Culture and Tourism for the permission to export the samples. This project has received funding from the European Research Council (ERC) under the European Union's Horizon 2020 research and innovation programme (grant agreement No. 647315 to NS). The funding organization had no influence in the study design, data collection and analysis, decision to publish, or preparation of the manuscript.

References

Ashkenazi, D., Taxel, I., Tal, O., 2015. Archaeometallurgical characterization of Late Roman- and Byzantine-period Samaritan magical objects and jewellery made of copper alloys. Mater. Charact. 102, 195–208.
Barber, D.J., Freestone, I.C., Moulding, K., Shortland, A.,.J., Reheren, T., Freestone, I.,.C., 2009. Ancient copper red glasses: investigation and analysis by micro-beam techniques. From Mine to Microscope. Advances in the Study of Ancient Technology. Vol. 2009, pp. 115–127.
Bayley, J., Freestone, I., Jackson, C. (Eds.), 2015. Glass of the Roman World. Oxbow, Oxford.
Biron, I., Chopinet, M.H., 2013. Colouring, decolouring and opacifying of glass. In: Janssens, K. (Ed.), Modern Methods for Analysing Archaeological and Historical Glass. Wiley, New York, pp. 49–65.
Bonnerot, O., Ceglia, A., Michelides, D., 2016. Technology and materials of Early Christian Cypriot wall mosaics. J. Archaeol. Sci. Rep. 7, 649–661.
Brill, R.H., 1988. Scientific investigations of the Jalame glass and related finds. In: Weinberg, G.D. (Ed.), Excavations at Jalame: Site of a Glass Factory in Late Roman Palestine. University of Missouri, Columbia, pp. 257–291.
Brill, R.H., 1999. Chemical Analyses of Early Glasses: Volume 1 (Tables) and 2 (Catalogue) (Corning).
Ceglia, A., Cosyns, P., Nys, K., Terryn, H., Thienpont, H., Meulebroeck, W., 2015. Late Antique glass distribution and consumption in Cyprus: a chemical study. J. Archaeol. Sci. 61, 213–222.
Cholakova, A., Rehren, T., Freestone, I.C., 2016. Compositional identification of 6th c. AD glass from the Lower Danube. J. Archaeol. Sci. Rep. 7, 625–632.
Collon, D., 2007. Mosaic Tesserae. In: Postgate, J.N., Thomas, D.C. (Eds.), Excavations at Kilise Tepe, 1994–1998: from Bronze Age to Byzantine in Western Cilicia. McDonald Institute/British Institute at Ankara, pp. 511–515.
Conte, S., Chinni, T., Arletti, R., Vandini, e.M., 2014. Butrint (Albania) between Eastern and Western Mediterranean glass production: EMPA and LA-ICP-MS of Late Antique and early Medieval finds. J. Archaeol. Sci. 49, 6–20.
Cutler, A., 2002. The industries of art. In: Laiou, A.E. (Ed.), The Economic History of Byzantium from the Seventh Through the Fifteenth Century, Vol. 2, Washington, pp. 555–587.
Degryse, P., 2014. Glass Making in the Graeco-Roman World. Leuven University Press, Leuven.
DeLaine, J., 1997. The Baths of Caracalla (Journal of Roman Archaeology Supplementary Series 25), Portsmouth.
Fiori, C., Vandini, M., Mazzotti, V., 2004. I colori del vetro antico. Il vetro musivo bizantino, Padua.
Foster, H.E., Jackson, C.M., 2009. The composition of late Romano-British colourless vessel glass: glass production and consumption. J. Archaeol. Sci. 37, 3068–3080.
Foy, D., Picon, M., Vichy, M., Thirion-Merle, V., 2003. Caractérisation des verres de la fin de l'Antiquité en Méditerranée occidentale: l'émergence de nouveaux courants commerciaux. In: Foy, D., Nenna, M.-D. (Eds.), Échanges et commerce du verre dans le monde antique: actes du colloque de l'Association française pour l'archéologie du verre, Aix-en-Provence et Marseille, 7–9 juin 2001. Éditions Monique Mergoil, Montagnac, pp. 41–85.
François, V., Spieser, J.-M., 2002. Pottery and glass in Byzantium, in: Laiou, A.E. (Ed.), The economic history of Byzantium from the Seventh Through the Fifteenth Century, Vol. 2. Washington, pp. 593–610.
Freestone, I.C., 1987. Composition and microstructure of early opaque red glass. In: Bimson, M., Freestone, I.C. (Eds.), Early Vitreous Materials. Britisg Museum Occasional Paper 56. British Museum, London, pp. 173–191.
Freestone, I.C., 1993. Theophilus and the composition of medieval glass. Mater. Res. Soc. Symp. Proc. 267, 739–745.
Freestone, I.C., 2015. The recycling and reuse of Roman glass: analytical approaches. Journal of Glass Studies 57, 29–40.
Freestone, I.C., Bimson, M., Buckton, D., 1990. Compositional categories of Byzantine glass tesserae. Annales du 11e Congrès de l'Association Internationale pour l'histoire du verre (Basel 1988). Amsterdam, pp. 271–279.
Freestone, I.C., Gorin-Rosen, Y., Hughes, M.J., 2000. Primary glass from Israel and the production of glass in late antiquity and the Early Islamic period. In: Nenna, M.-D. (Ed.), La route du verre. Ateliers primaires et secondaires du second millénaire av. J.C. au Moyen Âge. Maison de l'Orient Méditerranéen-Jean Pouilloux, Lyon, pp. 65–83.
Freestone, I.C., Stapleton, C.P., Rigby, V., 2003. The production of red glass and enamel in the Late Iron Age, Roman and Byzantine periods. In: Entwistle, C. (Ed.), Through a Glass Brightly. Studies in Byzantine and Medieval art and archaeology presented to David Buckton. Oxbow, Oxford, pp. 142–154.
Freestone, I.C., Jackson-Tal, R.E., Tal, O., 2008. Raw glass and the production of glass vessels at late Byzantine Apollonia-Arsuf, Israel. Journal of Glass Studies 50, 67–80.
Freestone, I.C., Jackson-Tal, R.E., Taxel, I., Tal, O., 2015. Glass production at an early Islamic workshop in Tel Aviv. J. Archaeol. Sci. 62, 45–54.
Gallo, F., Marcante, A., Silvestri, A., Molin, G., 2014. The glass of the "Case delle Bestie Ferite": a first systematic archaeometric study on Late Roman vessels from Aquileia. J. Archaeol. Sci. 41, 7–20.
Gliozzo, E., Turchiano, M., Giannetti, F., Memmi, I., 2016. Late antique and early medieval glass vessels from Fragola (Italy). Archaeometry 58 (Supplement S1), 113–147.
Gliozzo, E., Santagostino Barbone, A., Turchiano, M., Memmi, I., Volpe, G., 2012. The coloured tesserae decorating the vaults of the Fragola Balneum (Ascoli Satriano, Foggia, southern Italy). Archaeometry 54, 311–331.
Gratuze, B., 2012. Les verres mosaiqués du secteur de la maison de la Rotonde. Composition chimique et chrono-typologie. In: Balmelle, C., Bourgeois, A., Broise, H., Darmon, J.P., Ennaifer, M. (Eds.), Carthage, colline de l'Odéon, maison de la Rotonde et Cryptoportique. Ecole Française de Rome, pp. 797–801.
Gratuze, B., 2014. Application de la spectrométrie de masse à plasma avec prélèvement par ablation laser (LA-ICP-MS) à l'étude des recettes de fabrication et de la circulation des verres anciens. In: Dillmann, P., Bellot-Gurlet, L. (Eds.), Circulation des matériaux et des objets dans les sociétés anciennes. Collection Sciences Archéologiques, Paris, Éditions Archives Contemporaines, pp. 259–291.
Gratuze, B., 2016. Glass characterization using laser ablation-inductively coupled plasma-mass spectrometry methods. In: Dussubieux, L., Golitko, M., Gratuze, B. (Eds.), Recent Advances in Laser Ablation ICP-MS for Archaeology, Series: Natural Science in Archaeology. Heidelberg, Springer, Berlin, pp. 179–196.
Gratuze, B., Soulier, I., Barrandon, J.N., Foy, D., 1992. De l'origine du cobalt dans les verres. Revue d'archéométrie. 16, pp. 97–108.
Greenhalgh, M., 1989. The Survival of Roman Antiquities in the Middle Ages, London.
Jackson, M.P.C., 2007. The church. In: Postgate, J.N., Thomas, D.C. (Eds.), Excavations at Kilise Tepe, 1994–1998: from Bronze Age to Byzantine in Western Cilicia. McDonald Institute/British Institute at Ankara, pp. 185–197.
Jackson, M.P.C., 2013. Byzantine settlement at Kilise Tepe in Göksu Valley. In: Hoff, M.C., Townsend, R.F. (Eds.), Rough Cilicia. New historical and archaeological approaches. Proceedings of an International Conference held at Lincoln, Nebraska, October 2007. Oxbow, Oxford, pp. 219–232.
Jackson, M.P.C., 2015. 2007–2011 Excavations at Kilise Tepe: a Byzantine Rural Settlement in Isauria. 69. Dumbarton Oaks Papers, pp. 355–380.
James, L., 2006. Byzantine glass mosaic tesserae: some material considerations. Byzantine and Modern Greek Studies 30 (1), 29–47.
James, L., Soproni, E., Bjornholt, B., 2013. Mosaics by numbers. Some preliminary evidence from the Leverhulme database. In: Entwistle, C., James, L. (Eds.), New Light on Old Glass: Recent Research on Byzantine Mosaics and Glass. British Museum, London, pp. 310–328.
Jochum, K.P., Weis, U., Stoll, B., Kuzmin, D., Yang, Q., Raczek, I., et al., 2011. Determination of reference values for NIST SRM 610–617 glasses following ISO guidelines. Geostand. Geoanal. Res. 35 (4), 397–429.
Kamber, B.S., Greig, A., Collerson, K.D., 2005. A new estimate for the composition of weathered young upper continental crust from alluvial sediments, Queensland, Australia. Geochim. Cosmochim. Acta 69, 1041–1058.
Keller, D., 2006. Deposition, disposal and re-use of broken glass from early Byzantine churches. Annales du 17e congrès de l'Association Internationale pour l'Histoire du Verre, Anvers, 2006. Brussels, pp. 281–288.
Lachin, M.T., Serra, C.L., Silvestri, A., Molin, G.M., 2009. Vitreous mosaic from Tyana (Cappadocia). In: Lafli, E. (Ed.), Late Antique/early Byzantine Glass in the Eastern Mediterranean. Izmir, pp. 171–183.
Lahanier, C., 1987. Etudes des tesselles de mosaïques et de verre à vitre syriens. In: Canivet, M.T., Canivet, P. (Eds.), Huarte, sanctuaire chrétien d'Apamène: IVe-VIe s. (Bibliothèque archéologique et historique 122). Paris, pp. 331–346.
Lahlil, S., Biron, I., Galoisy, L., Morin, G., 2008. Rediscovering ancient glass technologies through the examination of opacifier crystals. Appl. Phys. A Mater. Sci. Process. 92, 109–116.
Lahlil, S., Biron, I., Galoisy, L., Morin, G., 2009. Technological processes to produce antimonite opacified glass throughout history. Annales du 17e Congrès de l'Association Internationale pour l'Histoire du Verre (Anvers, septembre 2006). Bruxelles, pp. 571–578.
Maltoni, S., Silvestri, A., 2016. Innovation and tradition in the fourth century mosaic of the Casa delle Bestie Ferite in Aquileia, Italy: archaeometric characterisation of the glass tesserae. Journal of Anthropological and Archaeological Science http://dx.doi.org/10.1007/s12520-016-0359-3.
Marii, F., 2013. Glass tesserae from the Petra Church. In: Entwistle, C., James, L. (Eds.), New Light on Old Glass: Recent Research on Byzantine Mosaics and Glass. British Museum, London, pp. 11–18.
Marii, F., Rehren, T., 2009. Archaeological coloured glass cakes and tesserae from the Petra Church. Annales du 17e Congrès de l'Association Internationale pour l'Histoire du Verre (Anvers, septembre 2006). Bruxelles, pp. 295–300.
Mass, J.L., Stone, R.E., Wypyski, M.T., 1998. The mineralogical and metallurgical origins of Roman opaque colored glasses. In: Kingery, W.D., McCray, P. (Eds.), The Prehistory

and History of Glassmaking Technology, Ceramics and Civilization. The American Ceramic Society, Ohio, pp. 121–144.
Moretti, C., Hreglich, S., 1984. Opacification and colouring of glass by the use of "anime". Glass Technol. 25 (6), 277–282.
Moropoulou, A., Zacharias, N., Delegou, E.T., Maroti, B., Kasztovszky, Z., 2016. Analytical and technological examination of glass tesserae from Hagia Sophia. Microchem. J. 125, 170–184.
Nakai, I., Numako, C., Hosono, H., Yamasaki, K., 1999. Origin of the red color of Satsuma copper-ruby glass as determined by EXAFS and optical absorption spectroscopy. J. Am. Ceram. Soc. 82, 689–784.
Neri, E., 2016. Tessellata vitrea in età tardoantica e altomedievale: produzione dei materiali e loro messa in opera. Considerazioni generali e studio dei casi milanesi. Brepols, Turnhout.
Neri, E., Verità, M., 2013. Glass and metal analyses of gold leaf tesserae from 1st to 9th century mosaics. A contribution to technological and chronological knowledge. J. Archaeol. Sci. 40, 4596–4606.
Neri, E., Conventi, A., Verità, M., 2013. Glass mosaic tesserae from the 5th-6th century baptistery of San Giovanni alle Fonti, Milan, Italy. Analytical investigations. In: Entwistle, C., James, L. (Eds.), New Light on Old Glass: Recent Research on Byzantine Mosaics and Glass. British Museum, London, pp. 1–10.
Neri, E., Biron, I., Verità, M., 2016. A Lost Mosaic (6th–9th c.) from Hierapolis (Turkey): PIXE/PIGE and SEM/EDS Analysis of Glass Tesserae (forthcoming).
Neri, E., Verità, M., Biron, I., Guerra, M.F., 2016. Glass and gold: Analyses of 4th–12th centuries Levantine mosaic tesserae. A contribution to technological and chronological knowledge. J. Archaeol. Sci. 70, 158–171.
Newton, R., Davison, D., 1999. Conservation of Glass. Butterworths, Oxford.
O'Hea, M., 2016. The glass (1998–2006). In: Joukowsky, M. (Ed.), Petra Great Temple Volume 3, Brown University Excavations 1993–2008, Architecture and Material Culture. Oxbow Books, Oxford, pp. 267–296.
Ponting, M.J., 1999. East meets West in post-classical Bet She'an: the archaeometallurgy of culture change. J. Archaeol. Sci. 26, 1311–1321.
Postgate, J.N., Thomas, D.C. (Eds.), 2007. Excavations at Kilise Tepe, 1994–1998: from Bronze Age to Byzantine in Western Cilicia, 2 Vols. McDonald Institute/British Institute at Ankara.
Rosenow, D., Rehren, T., 2014. Herding cats: Roman to late antique glass groups from Bubastis, northern Egypt. J. Archaeol. Sci. 49, 170–184.
Santagostino Barbone, A., Gliozzo, E., Turchiano, M., D'Acapito, F., Memmi Turbanti, I., Volpe, G., 2008. The *sectilia* panels of Faragola (Ascoli Satriano, southern Italy): a multi-analytical study of the red, orange and yellow glass slabs. Archaeometry 50, 451–473.
Schibille, N., McKenzie, J., 2014. Glass tesserae from Hagios Polyeuktos, Constantinople: their early Byzantine affiliations. In: Keller, D., Price, J., Jackson, C. (Eds.), Neighbours and Successors of Rome: Traditions of Glass Production and Use in Europe and the Middle East in the Later 1st Millennium AD. Oxbow Books, Oxford, pp. 114–127.
Schibille, N., Degryse, P., Corremans, M., Specht, C.G., 2012. Chemical characterisation of glass mosaic tesserae from sixth-century Sagalassos (south-west Turkey): chronology and production techniques. J. Archaeol. Sci. 39, 1480–1492.
Schibille, N., Sterrett-Krause, Freestone, I.C., 2016a. Glass groups, glass supply and recycling in Late Roman Carthage. Archaeol. Anthropol. Sci. 1-19.
Schibille, N., Meek, A., Tobias, B., Entwistle, C., Avisseau-Broustet, M., Da Mota, H., Gratuze, B., 2016b. Comprehensive chemical characterisation of byzantine glass weights. PLoS One 11 (12), e0168289. http://dx.doi.org/10.1371/journal.pone.0168289.
Shugar, A.N., 2000. Byzantine opaque red glass tesserae from Beit Shean, Israel. Archaeometry 42 (2), 375–384.
Silvestri, A., Tonietto, S., Molin, G., 2011. The palaeo-Christian glass mosaic of St. Prosdocimus (Padova, Italy): archaeometric characterisation of 'gold' tesserae. J. Archaeol. Sci. 38, 3402–3414.
Silvestri, A., Tonietto, S., Molin, G.M., Guerriero, P., 2012. The palaeo-Christian glass mosaic of St. Prosdocimus (Padova, Italy): archaeometric characterisation of tesserae with antimony- or phosphorus-based opacifiers. J. Archaeol. Sci. 39, 2177–2190.
Silvestri, A., Tonietto, S., Molin, G., Guerriero, P., 2014. The palaeo-Christian glassmosaic of St. Prosdocimus (Padova, Italy): archaeometric characterisation of tesserae with copper- or tin-based opacifiers. J. Archaeol. Sci. 42, 51–67.
Silvestri, A., Nestola, F., Peruzzo, L., 2016. Multi-methodological characterisation of calcium phospate in late-Antique glass mosaics tesserae. Microchem. J. 124, 811–818.
Tal, O., Jackson-Tal, R.E., Freestone, I.C., 2004. New evidence of the production of raw glass at late byzantine Apollonia-Arsuf, Israel. Journal of Glass Studies 46, 51–66.
Tite, M., Pradell, T., Shortland, A., 2008. Discovery, production and use of tin-based opacifiers in glasses, enamels and glazes from the late Iron Age onwards: a reassessment. Archaeometry 50 (1), 67–84.
Turner, W.E.S., Rooksby, H.P., 1959. A study of opalising agents in ancient opal glasses throughout three thousand four hundred years. Glastech. Ber. 17–28.
Uboldi, M., Verità, M., 2003. Scientific analyses of glasses from late Antique to early Medieval archaeological sites in northern Italy. Journal of Glass Studies 45, 115–137.
Verità, M., 2010. Glass mosaic tesserae of the Neonian Baptistry in Ravenna: nature, origin, weathering causes and processes. In: Fiori, C., Vandini, M. (Eds.), Ravenna Musiva. Ravenna, pp. 89–103.
Verità, M., 2016. I materiali vitrei dei mosaici parietali a Roma tra IV e XIII secolo: tecnologia e degrado, in I mosaici di Roma, a cura di M. Andaloro. Restauro, Roma, Istituto centrale del (in press).
Verità, M., Santopadre, P., 2010. Analysis of gold-colored ruby glass tesserae in Roman church mosaics of the fourth to 12th centuries. Journal of Glass Studies 52, 11–24.
Verità, M., Arena, M.S., Carruba, A.M., Santopadre, P., 2008. Materiali vitrei nell'opus sectile di Porta Marina (Ostia antica). Bollettino ICR. 16–17, pp. 78–94.
Verità, M., Maggetti, M., Saguì, L., Santopadre, P., 2013. Colors of Roman glass: an investigation of the yellow sectilia in the Gorga Collection. Journal of Glass Studies 55, 21–34.
Vicenzi, E.P., Eggins, S., Logan, A., Wysoczanski, R., 2002. Microbeam characterization of corning archeological reference glasses: new additions to the smithsonian microbeam standard collection. J. Res. Natl. Inst. Stand. Technol. 107 (6), 719.
Wagner, B., Nowak, A., Bulska, E., Hametner, K., Günther, D., 2012. Critical assessment of the elemental composition of corning archeological reference glasses by LA-ICP-MS. Anal. Bioanal. Chem. 402 (4), 1667–1677.
Werner, A.E., Bismon, M., 1967. Technical report on the glass gaming-pieces. In: Stead, I.M. (Ed.), A La Tène III burial at Welwyn Garden City. Archaeologia. 101, pp. 16–17.
Wypyski, M.T., 2005. Technical Analysis of Glass Mosaic Tesserae from Amorium. 59. Dumbarton Oaks Papers, pp. 183–192.
Wypyski, M.T., Becker, L., 2004. Glassmaking technology at Antioch. In: Becker, L., Kondoleon, C. (Eds.), The Arts of Antioch. Worcester, pp. 115–175.